Disentangling Complexity in Bayesian Automatic Adaptive Quadrature

Gheorghe Adam[1,2,⋆] and *Sanda* Adam[1,2,⋆⋆]

[1] *Laboratory of Information Technologies, Joint Institute for Nuclear Research, 6, Joliot Curie St., 141980 Dubna, Moscow Region, Russia*
[2] *Horia Hulubei National Institute for Physics and Nuclear Engineering (IFIN-HH), 30, Reactorului St., Măgurele – Bucharest, 077125, Romania*

Abstract. The paper describes a Bayesian automatic adaptive quadrature (BAAQ) solution for numerical integration which is simultaneously robust, reliable, and efficient. Detailed discussion is provided of three main factors which contribute to the enhancement of these features: (1) refinement of the *m*-panel automatic adaptive scheme through the use of integration-domain-length-scale-adapted quadrature sums; (2) fast early problem complexity assessment – enables the non-transitive choice among three execution paths: (i) immediate termination (exceptional cases); (ii) pessimistic – involves time and resource consuming Bayesian inference resulting in radical reformulation of the problem to be solved; (iii) optimistic – asks exclusively for subrange subdivision by bisection; (3) use of the weaker accuracy target from the two possible ones (the input accuracy specifications and the intrinsic integrand properties respectively) – results in maximum possible solution accuracy under minimum possible computing time.

1 Introduction

The present paper reports results along the lines of our recent investigations [1, 2] concerning the Bayesian automatic adaptive quadrature (`BAAQ`) solution [3] of definite Riemann integrals.

The essential requirements to the `BAAQ` algorithms are robustness, reliability, and efficiency under floating point computations. Their implementation asks for three main `BAAQ` developments.

(a) The refinement of the *m*-panel scheme of the standard adaptive quadrature (described, e.g., in [4–7]). This development was suggested by the fact that, under floating point computations, the algebraic degree of precision of an interpolatory quadrature sum ceases to be a characteristic invariant feature of it. The floating point degree of precision is the adequate quantity characterizing a quadrature sum [8]. A convenient way of taking into account this floating point feature was [1] to modify the *m*-panel scheme by the definition of three classes of integration domain length scales: *macroscopic, mesoscopic*, and *microscopic* and to use characteristic quadrature sums over each scale.

(b) The fast early problem complexity assessment is a new undertaking the need of which follows from the empirical fact that a single algorithm cannot efficiently cope with the myriad of existing

⋆ e-mail: adamg@jinr.ru,adamg@theory.nipne.ro
⋆⋆ e-mail: adams@jinr.ru,adams@theory.nipne.ro

Riemann integrals. However, instead of leaving with the user the expert decision on the choice among the large number of existing computing codes for numerical solution of the integrals (see, [4–7]), an attempt was made to investigate the possibility to define decision paths based on Bayesian inferences which are tailoring automatically the best way to follow to the derivation of accurate output.

(c) Finally, new results are reported concerning the code optimization in connection with the user accuracy requirements. A useful by-product of the problem complexity assessment is the possibility to define an integrand adapted upper accuracy target. Whenever this is less stringent than the target following from the user defined accuracy requirements, the latter is superseded by the former one. This decision has two desirable effects: it provides at output the best possible accuracy for the problem at hand, while sparing the unnecessary computations done beyond the maximum available accuracy.

With this general plan in mind, the discussion below is organized in four sections. Section 2 provides a summary of the `BAAQ` approach enabling independent lecture of this paper. Section 3 adds progress to the three class m-panel scheme proposed in [1]. Section 4 describes in detail the complexity assessment over macroscopic ranges. It also summarizes the integrand induced accuracy limitations. The paper ends with concluding remarks in section 5.

2 Summary of the Bayesian automatic adaptive quadrature

A `BAAQ` numerical solution of the (proper or improper) Riemann integral

$$I \equiv I_{[a,b]}[f] = \int_a^b g(x)f(x)\,\mathrm{d}x\,, \qquad -\infty < a < b < \infty, \tag{1}$$

is sought under the assumption that the real valued *integrand function* $f(x)$ is continuous almost everywhere on $[a, b]$ such that (1) exists and is finite. Here the *weight function* $g(x)$ either absorbs an analytically integrable difficult factor in the integrand (e.g., endpoint singularity or oscillatory function), or else $g(x) \equiv 1,\ \forall x \in [a, b]$.

Following [1], the subsequent `BAAQ` developments implement a solution of (1) within a *class dependent* m-panel rule approach. We remind that the m-panel rule idea was proposed within the standard automatic adaptive quadrature (`AAQ`) (see, e.g., [4–6]) as a means to adjust the discretization of the original integration domain $[a, b]$ to the rate of variation of $f(x)$ inside $[a, b]$. Within `AAQ`, over any integration range $[\alpha, \beta] \subseteq [a, b]$, a *fixed quadrature rule* is used irrespective of the width of $[\alpha, \beta]$.

The quadrature rule yields an $[\alpha, \beta]$ – dependent pair $\{q, e > 0\}$ where $q \equiv q_{[\alpha,\beta]}[f]$ denotes an approximation of $I_{[\alpha,\beta]}[f]$ produced by an *interpolatory quadrature sum*, while $e \equiv e_{[\alpha,\beta]}[f]$ denotes the *error estimate* associated to q, which is intended to provide an upper bound to the modulus of the remainder $r_{[\alpha,\beta]}[f] = I_{[\alpha,\beta]}[f] - q_{[\alpha,\beta]}[f]$. As pointed out in [1], the quadrature sum q is to be computed by *different* quadrature sums over three classes of integration domain widths: *macroscopic, mesoscopic*, and *microscopic*, respectively.

An `AAQ` algorithm works iteratively. The quadrature rule at hand provides a global output *initialization* $\{Q_N, E_N | N = 1\}$ over $[a, b]$. If the obtained approximation Q_1 of (1) is not accurate enough, then global output *refinement* is obtained by gradual subdivision of $[a, b]$ into subranges $[x^{i-1}, x^i] \subset [a, b];\ i = 1, 2, \ldots, N;\ N > 1$, over which *local outputs* $\{q_i, e_i > 0\}$ are computed. The summation of the local outputs over the existing subranges results in a *global output* update $\{Q_N, E_N > 0\}$. After each derived global output $\{Q_N, E_N | N \geq 1\}$, the fulfilment of the *global termination criterion* is checked [4],

$$|I - Q_N| < E_N < \max\{\varepsilon_a, \varepsilon_r |I|\} \simeq \max\{\varepsilon_a, \varepsilon_r |Q_N|\}, \tag{2}$$

where, ε_a and ε_r denote the *absolute accuracy*, respectively *relative accuracy* requested at input.

The termination of the iterative process may end successfully, or it may not. The reason for failure is the evaluation of local error estimates by use of *probabilistic arguments* which might result in one or more persistently spurious e_i values.

The BAAQ advancement to the solution rests on Bayesian inference based on four pillars: the theory of the Riemann integral, the theory of the numerical integration (quadrature), features of the floating point computation, the accumulated empirical evidence. Essentially, the probabilistic character of the AAQ approach to the derivation of local error estimates $e > 0$ is preserved. However, each step of the gradual advancement to the solution is scrutinized based on a set of hierarchically ordered criteria which enable decision taking in terms of the established diagnostics [3].

3 Refinement of the m-panel AAQ scheme

The inadequacy of the algebraic degree of precision for the characterization of the outputs of a quadrature sum in floating point computations [8] is illustrated in the figure 1.

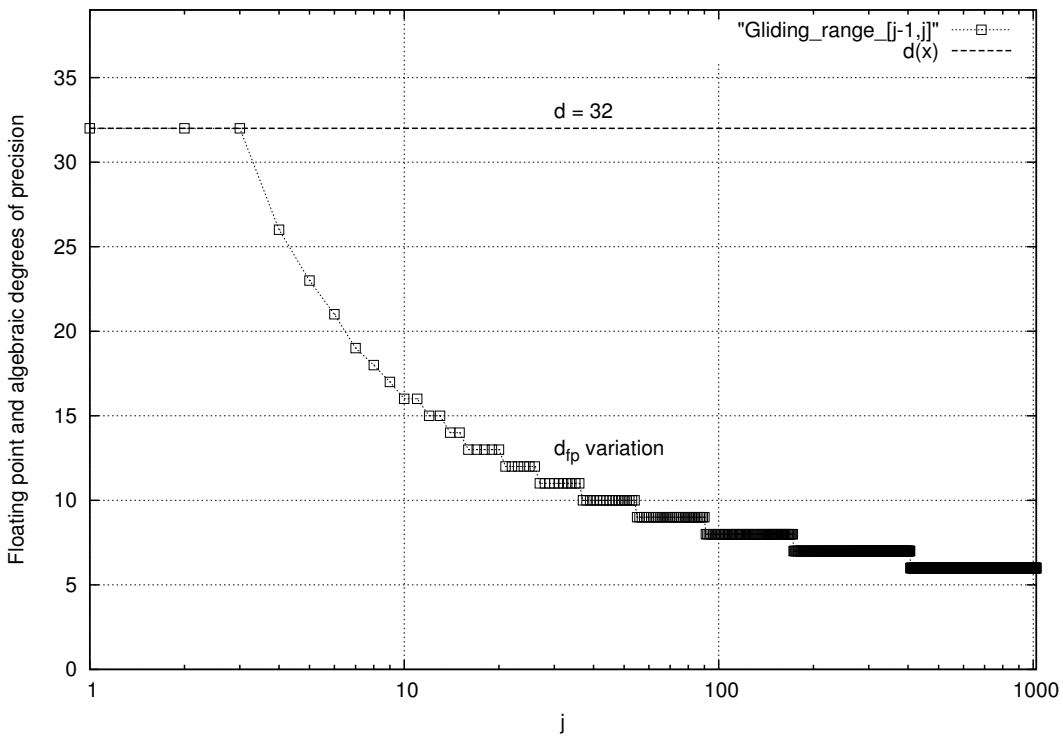

Figure 1. Variation of the floating point degree of precision of the CC-32 local quadrature rule over the gliding range $[0, 1]$ versus its distance $j - 1$ from the origin. It is found that $d_{\mathrm{fp}} = d = 32$ at low j values ($j = 1, 2, 3$), then d_{fp} abruptly decreases at larger but small enough j, to show slower decreasing rates under the displacement of $[0, 1]$ far away from the origin, and reaching a minimal value $d_{\mathrm{fp}} = 6$ at $407 \leq j \leq 1023$.

The quadrature sum of interest, abridged CC-32, implements Clenshaw-Curtis (CC) quadrature [9] at the 33-knot set at which the Chebyshev polynomial of the first kind and of polynomial degree 32 gets extremal values inside the standard reduced interval $[-1, 1]$. The CC-32 is of special interest

since it is the best choice [2] among the CC-like quadrature sums of algebraic degree of precision 2^m, $m \in \mathbb{N}^+$.

The evidence reported in fig. 1 contrasts the constant value ($d = 32$) of the algebraic degree of precision of the CC-32 and the dramatic variation of its floating point degree of precision in the case of the unit length range $[j-1, j]$ gliding along the real axis through integer values, $j = 1, 2, \ldots, 1023$.

Extensive numerical tests have confirmed the usefulness of the m-panel AAQ scheme refinement proposed in [1], concerning the definition of three length scales of the integration domain widths: *macroscopic, mesoscopic*, and *microscopic*, respectively.

However the *separation boundaries* between adjacent classes have been shifted toward larger values: $\tau_\mu = 2^{-20}$ (in-between microscopic and mesoscopic lengths) and $\tau_m = 2^{-6}$ (in-between mesoscopic and macroscopic lengths). The motivation stems from the need to start, over microscopic and mesoscopic length ranges, with computed integrand values over large enough sets of equally spaced quadrature knots. This enables a preliminary analysis of the complexity of the integral to be solved similar to that detailed below in the case of macroscopic ranges.

Over *ranges of microscopic length*, the minimal set of equally spaced quadrature knots is to consist of $2 \times 2 + 1 = 5$ elements. Over such a set, a two-term *composite Simpson rule* provides the reference quadrature sum output characterized by the highest possible algebraic degree of precision. The alternative knot grouping which consists of one central triplet for Simpson rule and two lateral doublets for composite trapezoidal rule yields a secondary composite quadrature sum output. From the difference of the two quadrature outputs and use of the triangle inequality rule, an associated error estimate results as a superposition of integrand curvatures at the three inner knots.

Over *ranges of mesoscopic length*, the use of a set of $4 \times 2 + 1 = 9$ equally spaced quadrature knots yields a reference quadrature sum from a two-term *composite 4-interval Newton rule.* Combination of a 4-interval Newton rule over the central knot quintuple with two lateral triplets for composite Simpson rule yields a secondary quadrature rule. Similar to the microscopic case, quadrature error estimates are obtained as a superposition of integrand curvatures at the seven inner knots.

Precision loss originating in cancellation by subtraction over microscopic and mesoscopic ranges.

As noticed in [1], the specification of the integration domain ends, which enters the standard input formulation provided by the equation (1), results in an *unavoidable precision loss* due to the cancellation by subtraction involved in the computation of the integration domain length as the difference of two (arbitrary) machine numbers sharing a set of common most significant digits.

If, however, the integration domain length is specified to machine accuracy either separately or within the definition of the integral to be solved, then no precision loss originating in cancellation by subtraction will happen.

4 Early Bayesian diagnostics over macroscopic ranges

4.1 Enhanced accuracy Clenshaw-Curtis Quadrature

The recent monograph [10] provides a detailed rigorous presentation of the attractive mathematical properties of the CC quadrature. In the frame of the BAAQ, the selection of the CC quadrature sums for the approximation of the Riemann integrals (1) over macroscopic integration ranges is motivated by several features of the spanning Chebyshev polynomials: closeness to the polynomials of the best approximation, symmetry properties, easiness of the analytic computation of the quadrature weights for different weight functions [4, 9, 11–13].

The interpolatory polynomial of the method is given by the truncated Chebyshev series expansion

$$L_n^\phi(y) = \sum_{k=0}^{n}{}'' b_k^n T_k(y), \tag{3}$$

(where the double prime shows that the first and the last terms of the sum are halved) of the reduced integrand

$$\phi(y) = f(c + hy), \quad c = (b + a)/2, \quad h = (b - a)/2, \quad y \in [-1, 1]. \tag{4}$$

$L_n^{\phi}(y)$ equates $\phi(y)$ at the set of $(n + 1)$ standard reduced CC quadrature knots

$$\{y_j^n = \cos(j\pi/n) \mid j = 0, 1, \ldots, n\}. \tag{5}$$

The computation of the Chebyshev expansion coefficients in (3) is the most computer intensive task of the method. The elucidation of the binary tree structures unveiling inheritance properties in the family of spanning Chebyshev polynomials of degrees $n = 2^m (m = 1, 2, \ldots)$ [2] allowed the derivation of a fast algorithm for the computation of these coefficients inside which the number of multiplications is kept at the lowest possible value.

The scrutiny of the derived algorithm has shown that the CC quadrature spanned by the 32-nd degree Chebyshev polynomial provides the best CC solution (rich integrand sampling and still economical algorithm). An undesirable feature of the reduction procedure (4) to the standard integration domain $[-1, 1]$ is the sizeable precision loss, due to the cancellation by subtraction, of the floating point values of the distances in-between neighbouring quadrature knots for the overwhelming fraction of the emerging pairs. This unfavourably impinges on the floating point accuracy of the divided differences entering the *integrand profile* (IP) analysis enabling Bayesian inferences [14].

The solution which avoids the above-mentioned precision loss is to use *modified reduced abscissas* (MRA), which are defined as distances of the standard reduced abscissas y_j^n to the nearest integration domain ends. The implementation of the MRA computation was done to machine accuracy. The computation of the distances between neighbouring MRA abscissas can be straightforwardly done, without precision loss by subtraction.

There is a set of 17 MRA entering the CC-32:

$$0 = \eta_0 < \eta_1 < \cdots < \eta_k < \cdots < \eta_{16} = 1, \quad \eta_{k+\mu} - \eta_{k+\mu-1} > \eta_k - \eta_{k-1}, \quad \mu > 0. \tag{6}$$

The price to be paid for this accuracy increase is the separate computation and storage into two separate vectors of the integrand values at MRA over the left and the right halves of an integration domain $[a, b]$ of width $h = (b - a)/2$: $f_k^l = f(a + h\eta_k)$; $f_k^r = f(b - h\eta_k)$; $k = 0, 1, \ldots, K = 16$, such that $f_{16}^l = f(a + h) = f_{16}^r = f(b - h)$.

4.2 Flow chart of early Bayesian inference

There are two main results established in this subsection: (1) the early Bayesian inference enables *consistent accommodation of the standard* AAQ *approach within the* BAAQ and (2) *robust termination criteria* are defined which efficiently stop the computations while returning optimum output for the input integral (with a problem defined accuracy ceiling which supersedes an unreachable ceiling following from the user accuracy requirements).

The flow chart below summarizes the eight steps of the proposed early Bayesian inference.

Input required:

- the accuracy parameter values $\varepsilon_a^{(i)}, \varepsilon_r^{(i)}$
- the integration domain (ID) $[a, b]$; its centre $c = (b + a)/2$; half width $h = (b - a)/2$
- the integrand function $f(x)$
- the MRA set $\{\eta_k\}$, computed to machine accuracy
- the computed integrand profile (IP) $\{(\eta_k, f_k^l) | k = 0, 1, \ldots, K = 16\} \cup \{(\eta_k, f_k^r) | k = 0, 1, \ldots, K = 16\}$

Main steps:

- **Step 0**: *Set grey diagnostic* (GD) *as default* (postponed decision)

- **Step 1**: *Integrand boundedness check over the input* IP enables:
  - Definition of extremal (max,min) integrand values, together with their location inside the IP
  - End of computation (EOC) under detection of exceptional cases: (computationally) constant integrand; odd integrand with respect to the ID centre $c = (b + a)/2$
- **Step 2**: If(.NOT.EOC) *Computation of Riemann sums over sublattices*
  - Two CC-32 sublattices are defined respectively by:
    - the 17 inherited CC-16 reduced abscissas (CC16)
    - the 16 newly added Fejer reduced abscissas (FJ16)
  - Pairs of Riemann sums over sublattices: $q_{\mathrm{CC16}}[(*)]$ and $q_{\mathrm{FJ16}}[(*)]$, where $(*)$ stays either for f or $|f|$
  - Riemann sum quadrature rule outputs for CC-32 IP:
    - trapezoidal rule quadrature sums: $q_{\mathrm{CC32}}[(*)] = (q_{\mathrm{CC16}}[(*)] + q_{\mathrm{FJ16}}[(*)])/2$
    - rough error estimates: $e_{\mathrm{CC32}}[(*)] = |q_{\mathrm{CC16}}[(*)] - q_{\mathrm{FJ16}}[(*)]|$
- **Step 3**: EOC *under detection of catastrophic cancellation by subtraction:* $|q_{\mathrm{CC32}}[(f)]| < \tau \cdot q_{\mathrm{CC32}}[|f|]$, τ close to machine epsilon with respect to addition.
- **Step 4**: If (.NOT. EOC) *check for problem dependent update of accuracy parameters* $\varepsilon_a^{(o)}, \varepsilon_r^{(o)}$
- **Step 5**: If (.NOT. EOC) decide on an *ill-conditioning* (IC) *diagnostic* iff
  - either $|q_{\mathrm{CC32}}[(f)]| < 2.0 \cdot q_{\mathrm{CC32}}[|f|]$
  - or $q_M > t_i \cdot q_m$, where $t_i \sim 100$ is an empirical threshold for the comparison of q_M with q_m , where $q_M = \max\{|q_{\mathrm{CC16}}[f]|, |q_{\mathrm{FJ16}}[f]|\}$ and $q_m = \min\{|q_{\mathrm{CC16}}[f]|, |q_{\mathrm{FJ16}}[f]|\}$
- **Step 6**: GD *diagnostic refinement* based on the outputs got for the Chebyshev series expansion coefficients
  - GD is changed to EOC iff negligible highest label even-rank and odd-rank CC-32 coefficients
  - GD is changed to IC iff either
    - (1) monotonicity is infringed for suitably chosen binary tree structure dependent subsets of CC-32 coefficients, or
    - (2) non-convergence or slow convergence is established to occurr for the CC-32 coefficients
- **Step 7**: *Check for further accuracy parameter updates*, $\varepsilon_a^{(o)}, \varepsilon_r^{(o)}$
- **Step 8**: *Path to subrange subdivision:*
  - If (IC) then define offending IP abscissas and refine IC diagnostic at these abscissas; subdivide current subrange into diagnostic-dependent finer subranges
  - elseif (GD) then proceed along the standard AAQ scheme.

4.3 Two illustrative examples

The accumulated empirical evidence plays a very important role in the decision taking process based on Bayesian inference. The data reported in [2] pointed to three different patterns of behaviour of the magnitudes of the Chebyshev expansion coefficients: *fast convergence* (suggesting rapid end of computations), *moderate convergence* (suggesting output improvement based on subrange bisection along the lines of the standard AAQ scheme), and *ill-conditioning* (irregular behaviour inside both the even-rank and the odd-rank coefficient subsets which is asking for IP analysis to resolve the offending integrand features).

The above-mentioned framework is refined by the scrutiny of the dependence of the even-rank (e) and odd-rank (o) Chebyshev expansion coefficients on the position of a singularity with respect to the ends of the current integration domain (figure 2).

Figure 2–left reports data for the integrand ([4], p.110) $f_1 : [0, 1] \to \mathbb{R}$, $f_1(x) = |x^2 + 2x - 2|^{-1/2}$, which shows an inner singularity at $x_s = \sqrt{3} - 1$.

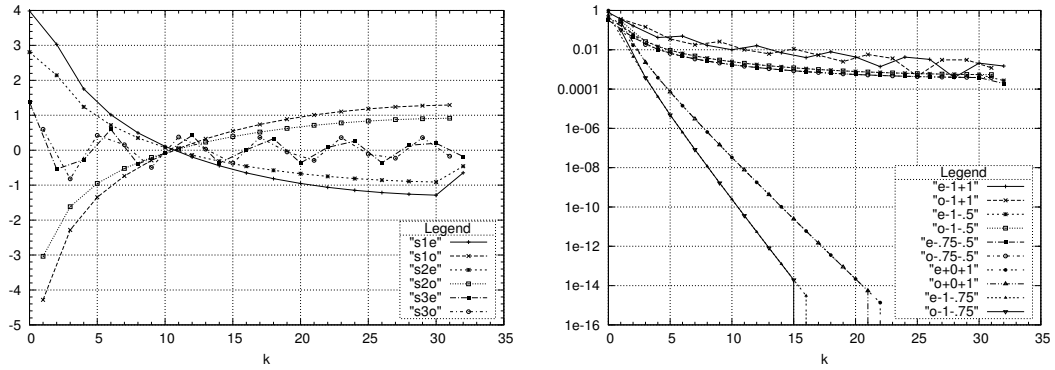

Figure 2. Patterns of variation of the Chebyshev expansion coefficients within the even and odd rank subsets versus the coefficient labels. In the file names in the left figure, "s" points to singular, "e" to even-rank coefficient subset, "3" to the subrange $[0, 1]$, "2" to the subrange $[x_s, 1]$, and "1" to the subrange $[x_s, \sqrt{3}/2]$. In the file names in the right figure "e" points to even-rank coefficient subset, "o" to odd-rank coefficient subset, the remaining figure pairs point to the left and the right ends of the subranges, respectively.

Figure 2–right reports outputs got for the integrand ([9]) $f_2 : [-1, 1] \to \mathbb{R}$, $f_2(x) = |x + 0.5|^{1/2}$, which shows an inner derivative singularity at $x_d = -0.5$.

The meanings of the notations used in the figure 2 are explained in the figure caption.

In the left figure, the behaviour of the "e" and "o" coefficient subsets over the range $[0, 1]$ is irregular due to the presence of an inner singularity at x_s, in agreement with [2]. In this case, an ill-conditioning diagnostic is issued at step 8 of Sec. 4.2, which is asking for the localization of the offending integrand feature to machine accuracy. However, for the ranges $[x_s, 1]$ and $[x_s, \sqrt{3}/2]$, both characterized by endpoint singularities, a *regular variation* of both the "e" and "o" coefficient subsets is noticed and this asks in the decision path for the activation of a convergence acceleration procedure.

The data in figure 2–right are given in semi-logarithmic scale. The behavioural patterns over the inner derivative singularity range $[-1, 1]$ as well as over the outer derivative singularity ranges $[0, 1]$ and $[-1, -0.75]$ are consistent with the data reported in Fig. 2–left and in [2]. The irregular behaviour pattern over the range $[-1, 1]$ asks for localization of the offending abscissa to machine accuracy. Over the ranges $[-1, x_d]$ and $[-0.75, x_d]$, characterized by endpoint derivative singularities, the noticed slowly converging monotonic behaviours of the coefficient subsets ask for the activation of the convergence acceleration procedure. Far from singularity (the other two cases), the good convergence properties shift the decision path to the standard `AAQ` scheme.

In both the left and right figures 2, the smaller the extension of the integration domain with an endpoint singularity, the larger are the ranges of variation of the two Chebyshev expansion coefficient subsets.

5 Conclusions

The present report discusses a Bayesian automatic adaptive quadrature (BAAQ) solution for numerical integration which is simultaneously robust, reliable, and efficient, yielding maximum possible output accuracy in numerical experiments under arbitrary behaviour of the integrand function.

An essential ingredient of the solution is the multiscale approach.

An early decision path to the integrand profile (IP) scrutiny enables the identification of trivial or manifestly unsolvable problems as well as the need to relax the user requested accuracy parameters.

Within the Clenshaw-Curtis quadrature over macroscopic ranges, the scrutiny of the Chebyshev expansion coefficients enable further identification of unresolved ill-conditioned features.

We are thus left either with a hopefully well-conditioned integral, for which the standard automatic adaptive quadrature can be used, or with a manifestly ill-conditioned problem for which an improved version of the full BAAQ machinery is activated.

Acknowledgement

Work supported within the Hulubei-Meshcheryakov Programme on 2017, JINR Orders 218/10.04.2017 (pp. 22, 23) and 219/10.04.2017 (pp. 93–95). The authors are grateful to an anonymous referee for the careful reading of the manuscript and his precise comments which helped improving details of the presentation.

References

[1] Gh. Adam and S. Adam, in Gh. Adam, J. Buša, and M. Hnatič (Eds.), MMCP 2015 *Mathematical Modeling and Computational Physics*, EPJ Web of Conferences **108**, 02002 (p1–p6) 2016, https://doi.org/10.1051/epjconf/201610802002

[2] S. Adam and Gh. Adam, in Gh. Adam, J. Buša, and M. Hnatič (Eds.), MMCP 2015 *Mathematical Modeling and Computational Physics*, EPJ Web of Conferences **108**, 02003 (p1–p6) 2016, https://doi.org/10.1051/epjconf/201610802003

[3] Gh. Adam and S. Adam, in *Mathematical Modeling and Computational Science* (MMCP2011), Gh. Adam, J. Buša, and M. Hnatič (Eds.) (Springer, Heidelberg, LNCS 7125, 2012) pp. 1–16

[4] R. Piessens, E. de Doncker-Kapenga, C. W. Überhuber, and D. K. Kahaner, `QUADPACK`*, a subroutine package for automatic integration* (Springer Verlag, Berlin, 1983)

[5] P.J. Davis and P. Rabinowitz, *Methods of Numerical Integration* (2-nd Ed., Academic Press, Orlando (Fla), USA, 1984)

[6] A.R. Krommer and C.W. Ueberhuber, *Computational Integration* (SIAM, Philadelphia, 1998)

[7] `NAG` *Library Manual*, Mark 24, section D01: http://www.nag.co.uk/numeric/fl/nagdoc_fl24/html/D01/d01conts.html (The Numerical Algorithms Group Ltd., Oxford, UK, 2012)

[8] S. Adam and Gh. Adam, in *Mathematical Modeling and Computational Science* (MMCP2011), Gh. Adam, J. Buša, and M. Hnatič (Eds.) (Springer, Heidelberg, LNCS 7125, 2012) pp. 189–194

[9] C.W. Clenshaw and A.R. Curtis, Numer. Math. **2**, 197–205 (1960)

[10] H. Brass and K. Petras, *Quadrature Theory. The Theory of Numerical Integration on a Compact Interval* (Math. Surv. and Monogr. vol. 178, American Mathematical Society, Providence, 2011)

[11] W.M. Gentleman, Comm. Assoc. Comp. Mach. **15**, 337–342, 343–346 (1972)

[12] R. Piessens and M. Branders, J. Comp. Appl. Math. **1**, 55, 153 (1975)

[13] Gh. Adam and A. Nobile, IMA J. Numer. Analysis **11**, 271–296 (1991)

[14] Gh. Adam and S. Adam, Numerical Methods and Programming: Advanced Computing **10**, 391–397 (2009) (http://num-meth.srcc.msu.ru/english/zhurnal/tom_2009/pdf/v10r145.pdf)